

1

2

3

4 **Fusion expression and anti-*Aspergillus flavus* activity of a novel inhibitory**
5 **protein DN-AflR**

6

7 **Yuan Liang, Qing Kong,[#] Yao Yao, Shujing Xu, Xiang Xie**

8

9 School of Food Science and Engineering, Ocean University of China, Qingdao,
10 Shandong, China

11

12

13

14

15

16 Running Title: Fusion expression of DN-AflR

17

18

19 [#]: Address correspondence to Qing Kong, kongqing@ouc.edu.cn.

20

21

22

23

24 **ABSTRACT** The regulatory gene (*aflR*) of aflatoxin encodes AfIR, a positive
25 regulator that activates transcriptional pathway of genes in aflatoxin biosynthesis.
26 New L-Asp-L-Asn (DN) extracted from *Bacillus megaterium* inhibited the growth of
27 *A. flavus* had been elucidated in our laboratory. The genes encoding DN and binuclear
28 zinc finger cluster protein of AfIR were fused, then fusion protein could compete with
29 the AfIS-AfIR complex for the AfIR binding site and significantly improve anti-*A.*
30 *flavus* activity of DN. The fusion gene *dn-aflR* was cloned into pET32a and
31 recombinant plasmid was introduced into *Escherichia coli* BL21. The highest
32 expression was observed after 10 h induction and purified by affinity chromatography
33 column. Compared with DN, the novel fusion protein DN-AfIR significantly inhibited
34 the growth of *A. flavus* and biosynthesis of aflatoxin B₁. This study promoted the use
35 of competitive inhibition of fusion proteins to reduce the expression of regulatory
36 genes in the biosynthetic pathway of aflatoxin. Moreover, it provided more supports
37 for deep research and industrialization of such novel, anti-*A. flavus* bio-inhibitors.

38 **IMPORTANCE** Aflatoxin contamination has seriously influence on export of
39 agricultural products, income of farmers and economic development. Biological
40 methods, especially using antagonistic microorganisms to inhibit aflatoxin
41 biosynthesis gradually become the hot spot in recent years. DN (L-Asp-L-Asn) from
42 *Bacillus megaterium*, which could inhibit growth of *Aspergillus flavus* and synthesis
43 of aflatoxin, has been identified. In this report, we fused the genes encoding inhibitory
44 peptides (DN) and specific zinc finger cluster protein, and expressed the novel anti-*A.*

45 *flavus* protein in *Escherichia coli*. Compared with DN, the inhibitory ability of novel
46 protein has been improved significantly. This research showed fusion expression of
47 anti-fungal proteins, such as DN-AflR, is a promising method to economically
48 improve the inhibitory activity of bio-inhibitors for *A. flavus*.

49

50 **KEYWORDS** AflR, *Aspergillus flavus*, *dn-aflR*, fusion expression

51

52 **INTRODUCTION**

53 Aflatoxin is one of the most potent naturally occurring toxic and carcinogenic
54 compound, which is a mycotoxin that poses a serious threat to human health (1).
55 Aflatoxin contamination has seriously influence on export of agricultural products,
56 income of farmers and economic development (2, 3). Biological methods, especially
57 using antagonistic microorganisms to inhibit aflatoxin biosynthesis gradually become
58 hot spot in recent years (4). Palumbo et al. isolated one strain of *Bacillus* from
59 almonds, which could inhibit the growth of *Aspergillus flavus* (5). Early studies found
60 that *Mycobacterium smegmatis* and *Rhodococcus erythropolis* could produce F420
61 H₂-dependent reductases to degrade aflatoxin (6, 7). Some studies isolated antifungal
62 compounds from *Bacillus* and verified their inhibitory effects on the growth of *A.*
63 *flavus* (8, 9). Above all, antagonistic microorganisms could produce metabolites or
64 enzymes to inhibit expression of regulatory genes, or degrade aflatoxin.

65 Aflatoxin biosynthetic pathway has been studied for years and is one of the best
66 understood fungal secondary metabolic pathways. The whole-genome sequencing of

67 *A. flavus* has been accomplished, and we could better control aflatoxin contamination
68 through deep research of the regulatory genes and mechanisms. Up to now, at least 34
69 genes have been identified as members of the aflatoxin pathway gene cluster. On the
70 82-kb biosynthetic gene cluster of aflatoxin, *aflR* and *aflS* (formerly known as *aflJ*)
71 are genes involved in pathway regulation (10, 11). *aflR* is necessary for transcription
72 of some genes in *Aspergillus* gene cluster (12-14). This gene encodes a specific DNA
73 binding protein (AflR) containing 444 amino acids, and the 29th to 56th amino acids
74 constitute a binuclear zinc finger cluster protein with sequence
75 Cys-Xaa2-Cys-Xaa6-Cys-Xaa6-Cys-Xaa2-Cys-Xaa6-Cys, which is the key region of
76 AflR to activate gene transcription and determines AflR-binding specificity (15). AflR,
77 which possesses DNA-binding and activation domains typical of the GAL4-type
78 family of positive regulatory proteins in yeast and fungi (16). A common feature of
79 fungal gene clusters, including those for secondary metabolites, is the presence of
80 specific regulatory genes, which have been found to encode members of the zinc
81 binuclear cluster protein family typified by GAL4 (17-19). AflS was found to be
82 involved in the regulation of transcription. Between *aflR* and *aflS* is intergenic region,
83 where promoter region is located. AflS-AflR complex binds to AflR binding site and
84 activates aflatoxin biosynthesis. Studies suggested that failure to product aflatoxin due
85 possibly to alternation in the interaction between AflS and AflR (10, 20).
86 Bio-inhibitors inhibited expression of *aflR* or *aflS* mainly by acting on the intergenic
87 region, thereby prevented the formation of AflS-AflR complex, so that AflS-AflR
88 complex could not bind to AflR binding site and activate biosynthetic pathway of

89 aflatoxin.

90 Recently, we identified DN (L-Asp-L-Asn) from *Bacillus megaterium*, which
91 could inhibit growth of *A. flavus* and synthesis of aflatoxin. To improve the inhibitory
92 effect of DN, we transformed the genes encoding DN and GAL4-type zinc finger
93 cluster protein (specifically binds to the AflR binding site) by gene fusion. We
94 hypothesized the fusion protein could compete with AflS-AflR complex by acting on
95 AflR binding sites to inhibit the activation of AflS-AflR complex and improve anti- *A.*
96 *flavus* activity of DN.

97

98 **RESULTS**

99 **Effects of DN on mycelia morphology of *A. flavus*. (i) TEM.** In control group,
100 the internal structure of cells grew normally and various organelles were clearly
101 visible (Fig. 2A and B). However, cell structures of mycelia treated by DN were
102 obviously abnormal: organelles were degenerated, and vacuole became significantly
103 larger, expanded and fractured (Fig. 2C and D).

104 **(ii) SEM.** Mycelia of control group were integrity, showing straight, neatly
105 arranged and smooth surface (Fig. 2E and F). While mycelia treated with DN grew
106 abnormally: mycelia were rough and had uneven thickness, and appeared to be
107 distorted and broken (Fig. 2G and H).

108 **Expression and identification of fusion protein.** The expected DNA and vector
109 fragments were seen in 1% agarose electrophoresis after digesting with EcoR I and

110 Hind III. Colony PCR and DNA sequencing showed that target fragment (*dn-afIR*)
111 was successful inserted into the vector. The molecular weight of empty plasmid
112 (Trx-His-pET32a) and fusion protein (Trx-His-DN-AfIR) were predicted to be 19 kDa
113 and 22 kDa. Expression vector with fusion gene had a distinct protein band (24 kDa,
114 Fig. 3A, lanes 1 and 2). The empty plasmid did not express the band at the
115 corresponding position and had its own specific band (Fig. 3A, lane 3). Results
116 illustrated successful expression of the fusion protein DN-AFLR. The supernatant
117 after ultrasonic breaking (Fig. 3B, lane 1) and the precipitate after 8 mM urea
118 dissolved (Fig. 3B, lane 2) both showed obvious protein bands. The result was
119 consistent with predicted weight of expected protein before purification (Fig. 3A).
120 There were no obvious protein bands in wash buffer (Fig. 3B, lanes 3-5), and there
121 was only one obvious protein band in elution buffer (Fig. 3B, lanes 6 and 7), which
122 corresponded to the target protein. ImageJ software (<https://imagej.nih.gov/ij/>) was
123 used to compare the density of the bands on the gel, the fusion protein accounts for
124 approximately 57.4% of the total cellular protein, the relative content of fusion protein
125 was about 600 $\mu\text{g ml}^{-1}$.

126 **Inhibitory effect of DN-AfIR on growth of *A. flavus*.** Plate treated by DN had
127 only a small inhibition zone of 5.0 ± 0.2 mm (Fig. 4A, plate a). The control group (Fig.
128 4A, plate c) and 200 mM imidazole treated group (Fig. 4A, plate b) showed no
129 significant zone of inhibition. Diameter of inhibition zone treated with fusion protein
130 was as high as 21.3 ± 0.2 mm (Fig. 4A, plates d-f). Inhibitory ability of DN-AfIR was
131 much stronger than that of DN. The MICs of DN-AfIR and DN were $150 \mu\text{g ml}^{-1}$ and

132 400 $\mu\text{g ml}^{-1}$, respectively. MFC of DN-AflR was 400 $\mu\text{g ml}^{-1}$. Results of two repeated
133 experiments were consistent (Table 1). The MIC and MFC of fusion protein were
134 lower than that of DN, indicating that the fusion protein had stronger inhibitory effect
135 on growth of *A. flavus* at a lower concentration.

136 **Inhibitory effect of fusion protein on aflatoxin B₁ biosynthesis.** Two groups of
137 experiments were performed using DN-AflR and DN with final concentrations of 30,
138 60, and 90 $\mu\text{g ml}^{-1}$. The residual rate of aflatoxin B₁ after fusion protein treatment was
139 24.37%, 14.21% and 6.74%, respectively, and the residual rate of aflatoxin B₁ after
140 DN treatment was 44.39%, 22.19% and 10.99%, respectively (Fig. 4B). Compared
141 with DN, fusion protein had stronger inhibitory effect on biosynthesis of aflatoxin B₁
142 ($P<0.05$). At 30 $\mu\text{g ml}^{-1}$ of DN-AflR, more than 75% aflatoxin B₁ was degraded.

143 **Physical properties and molecular structure of DN-AflR.** Amino acid
144 sequence, isoelectric point and other basic informations were analyzed by ExPASy
145 (<http://web.expasy.org/protparam/>; Table 2). Secondary structure of protein was
146 predicted by SPLIT (<http://splitbioinf.pmfst.hr/split/4/>; Fig. 5A). Spatial structure was
147 predict by SWISS-MODEL. The fusion protein DN-AflR carries a positive charge,
148 has a relative strong hydrophobic effect, and contains the characteristic secondary
149 structure of the protein. By analyzing the predicted structures of DN-AflR (Fig. 5B)
150 and GAL4 (Fig. 5C), DN-AflR has the zinc finger DNA-binding functional structure
151 (specifically binds to AflR binding site) (Fig. 5D).

152

153 **DISCUSSION**

154 At present, more and more microorganisms and their metabolites were reported to
155 inhibit the growth of *Aspergillus flavus* and degrade aflatoxins (5, 26). Albert et al.
156 transformed the laccase gene of *T. versicolor* into recombinant *A. niger* by gene
157 cloning, and the inhibition rate on aflatoxin of laccase (118 U L^{-1}) after recombinant
158 expression as high as 55% (27). Douillard et al. demonstrate that novel *L. lactis* fusion
159 partner expression vectors allow high-level expression of soluble heterologous
160 proteins (28). Study showed that Fh8 tag fusion expression could significantly
161 improve the ability of *E. coli* to express soluble exogenous proteins (29). Genetic
162 engineering could highly express the active proteins and other metabolites in
163 prokaryotic or eukaryotic hosts, which is the great way to cut down costs.

164 However, there was few report on the inhibition of growth of *A. flavus* by
165 molecular modification of positive regulatory genes in aflatoxin biosynthesis. Fusion
166 expression has been continuously applied to the process of expressing recombinant
167 protein in order to improve functions of the active protein (30, 31). TEM and SEM are
168 effective applications to analyze the characteristics and morphologies of samples.
169 SEM showed that DN caused changes in mycelial morphology of *A. flavus*. TEM
170 showed the ruptured vacuoles accounted for most of cell space and destroyed the
171 function and balance of other organelles, which affected normal growth of the whole
172 cell (Fig. 2). So that DN had the ability of inhibiting the growth of *A. flavus*.

173 In order to improve the anti-*A. flavus* effect of DN, we fused the genes encoding
174 DN and sequences of zinc finger cluster protein (specifically binds to the AfIR
175 binding site), then successfully constructed a recombinant plasmid dn-afIR-pET32a

176 (Fig. 1). In the process of *E. coli* expression, when expressed in the host system at a
177 high level, the recombinant protein was easy to form inclusion bodies (32). This may
178 be due to the fact that during the expression, the protein folded too fast, while
179 insufficient supply of enzymes or co-factors made it cannot form the correct
180 secondary bond. According to the reports (33), we used 16°C, 160 rpm as the
181 conditions for inducing expression. In general, target proteins with a molecular weight
182 of less than 5 kDa or more than 100 kDa could not be expressed easily. The smaller
183 molecular weight of protein, the easier it was to be degraded. In order to avoid
184 degradation of target protein due to its low molecular weight, we used the pET32a
185 vector to express the active protein, and its Trx and His tag significantly improved the
186 stability of expression, and enhanced purification of protein, respectively. Because
187 target protein contained the His tag, result of SDS-PAGE showed that molecular
188 weight of fusion protein was 24 kDa (Fig 3), which was a little more than the
189 predicted molecular weight by the theoretical calculations (20 kDa). Compared with
190 DN, the fusion protein DN-AflR had stronger inhibitory effect on growth of *A. flavus*
191 (Fig. 4A). Simultaneously, it also had significant advantages in inhibiting aflatoxin B₁
192 biosynthesis (Fig. 4B), especially, under 30 µg mL⁻¹ concentration of DN-AflR, more
193 than 75% aflatoxin B₁ was inhibited. To get a deeper comprehension of DN-AflR, its
194 physical properties and molecular structures were predicted. Outer membrane of most
195 cells is negatively charged, while most anti-fungal proteins are positively charged and
196 they can bind to the cells surface through electrostatic attraction (34). The α-helical
197 peptides with higher hydrophobic properties have a higher ability to lyse membranes,

198 and the inhibitory activity of some peptides would even disappear with reduced
199 hydrophobicity (35). Through the predicted results, the fusion protein DN-AflR
200 carries positive charge and has a relative strong hydrophobic effect, and contains the
201 secondary structure of helix. Especially, DN-AflR contains the zinc finger cluster
202 protein structure (compare with GAL4), which make it could compete with AflS-AflR
203 complex by acting on AflR binding sites to inhibit the activation of aflatoxin. These
204 properties confirmed that DN-AflR had high inhibitory ability on growth of *A. flavus*
205 and biosynthesis of aflatoxin.

206 To the best of our knowledge, this is the first report about fusing the genes
207 encoding inhibitory peptides and specific zinc finger cluster protein, and fusion
208 expressed the novel anti-*A. flavus* protein. Results showed the modified novel protein
209 reduced aflatoxin biosynthesis and growth of *A. flavus*, which could control aflatoxin
210 contamination. Compared with DN, the inhibitory ability of novel protein has been
211 improved significantly.

212 This work promoted deep researches for fusion expression of anti-fungal proteins.
213 Furthermore, this study also provided more theoretical basis and technical support for
214 the further biocontrol of *A. flavus* and a new idea about enhancing the anti-*A. flavus*
215 ability of inhibitory substances.

216

217 MATERIALS AND METHODS

218 **Materials, strains, and culture conditions.** *A. flavus* NRRL3357, preserved in

219 School of Food Science and Engineering, Ocean University of China, was maintained
220 at 4°C on potato dextrose agar (PDA; Bio-way technology, Shanghai, China). For
221 liquid culture, *A. flavus* was transferred into a 250 ml Erlenmeyer flask containing
222 100 ml of MM medium at 28°C. *Escherichia coli* DH5 α and *E. coli* BL21 (Ruibio
223 Biotech, Beijing, China) were used as hosts for plasmid amplification and genes
224 expression, respectively. *E. coli* was grown in LB medium (10 g l⁻¹ Tryoton, 5 g l⁻¹
225 Yeast Extract, 10 g l⁻¹ NaCl) containing 50 μ l ml⁻¹ ampicillin (Solarbio, Beijing,
226 China) at 37°C with shaking at 180 rpm.

227 **Effects of DN on mycelia morphology of *A. flavus*. (i) Preparation of spores**
228 **suspension.** Spores of *A. flavus* were washed off with sterile distilled water
229 containing 0.1% Tween-80 from PDA medium and filtered with a cotton slag to
230 prepare spores suspension. The number of spores was counted by haemocytometer
231 and diluted to the desired concentration.

232 **(ii) TEM and SEM.** 0.8 mg ml⁻¹ DN (synthesized in GL Biochem, Shanghai,
233 China) and 10⁵ spores ml⁻¹ were added in 50 ml MM medium and cultivated at 28°C
234 with 180 rpm for 48 h. Control group didn't contain DN. Then the mycelia were fixed
235 with 2.5% glutaraldehyde, dehydrated in ethanol and embedded in an epoxy resin to
236 be observed by Transmission Electron Microscope (TEM; JEOL, Tokyo, Japan) (21),
237 and the mycelia were also observed with Scanning Electron Microscope (SEM; JEOL,
238 Tokyo, Japan) after dispersion by ultrasonic wave (22).

239 **Expression and identification of fusion protein. (i) Expression vector and its**

240 **construction and transformation into *E. coli* BL21.** The fusion gene *dn-afIR*
241 containing genes encoding DN and zinc binuclear cluster protein
242 (Cys-Xaa2-Cys-Xaa6-Cys-Xaa6-Cys-Xaa2-Cys-Xaa6-Cys, based on AAM03003.1,
243 NCBI) was synthesized by Hongxun Biotech (Suzhou, China), and amplified with
244 PCR (forward primer 5'-GAATTCGACAACGACAACT-3', reverse primer 5'-
245 AAGCTTACAGGCAAGACCA-3'). Sequences for restriction site EcoR I were
246 sequentially incorporated at the 5'-end and Hind III restriction site was in order added
247 to the 3'-end, and extracted gene by Plasmid Mini Kit (OMEGA, Omega bio-tek,
248 Shanghai, China). Restriction enzymes Hind III and EcoR I were used to digest the
249 *dn-afIR* and pET32a (+), then the digested fragments were separated and identified on
250 1% agarose gel and recovered from gel using Agarose DNA Extraction Kit (OMEGA,
251 Omega bio-tek, Shanghai, China). The digested fragments were ligated at 4°C with T4
252 DNA ligase (Thermo Fisher Scientific, New York, USA) (Fig. 1). Then recombinant
253 plasmid *dn-afIR-pET32a* was transformed into *E. coli* DH5 α and single colony was
254 picked for colony PCR. The recombinant plasmid extracted from suspension and
255 empty plasmid were both transformed into *E. coli* BL21 by heat shock, and cultivated
256 on solid LB medium containing 50 $\mu\text{g ml}^{-1}$ ampicillin (23). After 16 h, single colony
257 was inoculated into LB liquid medium and sent it to Ruibio Biotech (Beijing, China)
258 for DNA sequencing.

259 **(ii) Protein expression and analysis.** A single colony (containing
260 *dn-afIR-pET32a*) was inoculated into 10 ml LB medium and cultured at 37°C. Then
261 overnight culture was inoculated into fresh 300 ml LB media in 1:5 ratio. When

262 optical density (OD₆₀₀) reached 0.6, the final concentration of 0.8 mM IPTG was
263 added to induce the expression. After 10 h induction at 16°C under 160 rpm, the cells
264 were washed with buffer (20 mM Tris, 30 mM NaCl, 10 mM imidazole, pH=7.5) and
265 then lysed by sonication (JY92-IIN, Ningbo Scientz Biotech, Ningbo, China;
266 ultrasonic power 300 w, ultrasound work 4 s, stop 6 s, 60 times). Supernatant was
267 collected and identified by SDS-PAGE.

268 **(iii) Protein purification.** The presence of a His tag in the recombinant protein
269 meant that the purification was performed with Ni²⁺-NTA affinity chromatography.
270 Briefly, samples were passed through a column and extensively washed with the
271 elution buffer (100 mM Tris base, 500 mM NaCl, and 200 mM Imidazole, pH=8).
272 Purified fusion protein was demonstrated by SDS-PAGE and relative quantity was
273 determined by Bradford protein assay in wave length of 595 nm by standard protein
274 BSA (bovine serum albumin) (Solarbio, Beijing, China).

275 **Effects of DN and DN-AflR on growth of *A. flavus*. (i) Anti-*A. flavus* activity.**

276 Fusion protein was evaluated by agar disk diffusion experiment. The diameter of
277 inhibition zone indicated the anti-*A. flavus* activity. 0.1 ml spores suspension (10⁵
278 spores ml⁻¹) was coated on PDA plate, and Oxford Cups filled with 100 µl DN (600
279 µg ml⁻¹) and DN-AflR (600 µg ml⁻¹) were put on it, respectively. The Oxford Cup on
280 control plate was filled with 100 µl sterile water.

281 **(ii) MIC and MFC.** A series of solutions containing DN-AflR or DN at the
282 concentrations of 30, 50, 100, 150, 400, 600 and 900 µg ml⁻¹ were prepared by serial
283 dilution. 200 µl of above solutions was added into each well of 96-well plates

284 containing PDA medium, respectively. Pure PDA without DN-AflR and DN was the
285 control. Then 5 μ l suspension (10^5 spores ml^{-1}) was added to each well and placed at
286 28°C for 48 h (24). By definition, the minimum concentration of compound that
287 completely inhibited growth of *A. flavus* was the minimum inhibitory concentration
288 (MIC) (non-visible *Aspergillus* hyphae); the culture was continued for 8 days to get
289 the MFC, while the lowest fungicidal concentration (MFC) was the lowest
290 concentration which no spore could germinate at.

291 **Effects of DN and DN-AflR on AFB₁ biosynthesis.** DN or DN-AflR (final
292 concentrations of 30, 60 and 90 $\mu\text{g ml}^{-1}$) were added into 30 ml MM medium,
293 respectively, and 100 μ l of suspension (10^5 spores ml^{-1}) was inoculated to each group
294 and incubated at 28°C with 200 rpm. Each experiment was repeated 3 times. After
295 culturing for 48 hours, samples were centrifuged at 8000 g for 20 min at room
296 temperature. Five milliliters of supernatant were diluted with 5 ml ultrapure water.
297 Next, 5 ml of the diluted sample was extracted in immune affinity columns (Huaan
298 Magnech BioTech Co., Ltd., Beijing, China) and then eluted with 1 ml of methanol at
299 a flow rate of 1 drop per second. The eluent was evaporated under a gentle stream of
300 nitrogen at 45°C up to dryness condition, and then derivatized with 200 μ l hexane and
301 100 μ l trifluoroacetic acid (TFA) for 15 min. After being evaporated to dryness again,
302 the eluent was redissolved in 200 μ l water–acetonitrile (85:15, v/v).

303 AFB₁ was analyzed according to retention time in HPLC system equipped with a
304 ZORBAX Eclipse XDB-C18 column (4.6 \times 150 mm, 5 μ m, Agilent, Palo Alto, CA,
305 USA) and a 470 fluorescent detector (G1321A, Agilent, USA) (λ_{exc} 360 nm; λ_{em}

306 440 nm) using a mobile phase solvent of 10% acetonitrile, 40% methanol, and 50%
307 water. The flow rate was 0.8 ml min⁻¹ and injection volume was 20 µl (25).

308 **Statistical analysis.** All data were presented as mean ± S.D. One-way analysis of
309 variance (ANOVA) and Duncan's multiple comparison test were used and carried out
310 with SPSS software (SPSS Inc., Chicago, IL, USA). $P < 0.05$ was considered
311 statistically significant.

312

313 **ACKNOWLEDGEMENTS**

314 We thank National Natural Science Foundation of China (31471657) and the
315 research grant from Qingdao Municipal Science and Technology Project
316 (16-6-2-39-nsh) for supporting this research.

317

318 **REFERENCES**

- 319 1. Cleveland TE, Yu JJ, Bhatngar D, Chen ZY, Brown RL, Chang KP, Cary GW.
320 2004. Progress in elucidating the molecular basis of the host plant–*Aspergillus*
321 *flavus* interaction: a basis for devising strategies to reduce aflatoxin
322 contamination in crops. *J Toxicol-Toxin Rev* 23:345-380.
- 323 2. Wu F, Guclu H. 2012. Aflatoxin regulations in a network of global maize trade.
324 *PLoS One* 7:e45151.
- 325 3. Atehnkeng J, Donner M, Ojiambo PS, Ikotun B, Augusto J, Cotty PJ,
326 Bandyopadhyay R. 2016. Environmental distribution and genetic diversity of
327 vegetative compatibility groups determine biocontrol strategies to mitigate
328 aflatoxin contamination of maize by *Aspergillus flavus*. *Microb Biotechnol*

- 329 9:75-88.
- 330 4. Mishra HN, Das C. 2010. A review on biological control and metabolism of
331 aflatoxin. *Crit Rev Food Sci* 43:245-264.
- 332 5. Palumbo JD, Baker JL, Mahoney NE. 2006. Isolation of bacterial antagonists of
333 *Aspergillus flavus* from almonds. *Microb Ecol* 52:45-52.
- 334 6. Taylor MC, Jackson CJ, Tattersall DB, French N, Peat TS, Newman J, Briggs LJ,
335 Lapalika GV, Campbell PM, Scott C, Russell RJ, Oakeshott JG. 2010.
336 Identification and characterization of two families of F420 H₂-dependent
337 reductases from Mycobacteria that catalyse aflatoxin degradation. *Mol Microbiol*
338 78:561-575.
- 339 7. Lapalika GV, Taylor MC, Warden AC, Scott C, Russell RJ, Oakeshott JG. 2012.
340 F420 H₂-dependent degradation of aflatoxin and other furanocoumarins is
341 widespread throughout the Actinomycetales. *PLoS One* 7:e30114.
- 342 8. Zhang T, Shi ZQ, Hu LB, Cheng LG, Wang F. 2008. Antifungal compounds from
343 *Bacillus subtilis* B-FS06 inhibiting the growth of *Aspergillus flavus*. *World J*
344 *Microb Biot* 24:783-788.
- 345 9. Bottone EJ, Peluso RW. 2003. Production by *Bacillus pumilus* (MSH) of an
346 antifungal compound that is active against *Mucoraceae* and *Aspergillus* species:
347 preliminary report. *J Med Microbiol* 52:69-74.
- 348 10. Cleveland TE, Yu JJ, Fedorova N, Bhatnagar D, Payne GA, Nierman WC,
349 Bennett JW. 2009. Potential of *Aspergillus flavus* genomics for applications in
350 biotechnology. *Trends Biotechnol* 27:151-157.

- 351 11. Yu JJ, Chang PK, Ehrlich KC, Cray JW, Bhatnagar D, Cleveland TE, Payne GA,
352 Linz JE, Woloshuk CP, Bennett JW. 2001. Clustered pathway genes in aflatoxin
353 biosynthesis. *Appl Environ Microbiol* 70:1253–1262.
- 354 12. Chang, PK, Ehrlich KC, Yu JJ, Bhatnagar D, Cleveland TE. 1995. Increased
355 expression of *Aspergillus parasiticus aflR*, encoding a sequence-specific
356 DNA-binding protein, relieves nitrate inhibition of aflatoxin biosynthesis. *Appl*
357 *Environ Microbiol* 61: 2372–2377.
- 358 13. Woloshuk CP, Foutz KR, Brewer JF, Bhatnagar D, Cleveland TE, Payne GA.
359 1994. Molecular characterization of *aflR*, a regulatory locus for aflatoxin
360 biosynthesis. *Appl Environ Microbiol* 60:2408–2414.
- 361 14. Matsushima K, Chang PK, Yu J, Abe K, Bhatnagar D, Cleveland TE. 2001.
362 Pre-termination in *aflR* of *Aspergillus sojae* inhibits aflatoxin biosynthesis. *Appl*
363 *Microbiol Biot* 55:585-589.
- 364 15. Burger G, Strauss J, Scazzocchio C, Lang BF. 1991. The pathway specific
365 regulatory gene of nitrate assimilation in *Aspergillus nidulans*, encodes a putative
366 GAL4-type zinc finger protein and contains four introns in highly conserved
367 regions. *Mol Cell Biol* 11:5746–5755.
- 368 16. Ehrlich KC, Montalbano BG, Cary JW. 1999. Binding of the C6-zinc cluster
369 protein, AFLR, to the promoters of aflatoxin pathway biosynthesis genes in
370 *Aspergillus parasiticus*. *Gene* 230:249-257.
- 371 17. Marmorstein R, Carey M, Ptashne M, Harrison SC. 1992. DNA recognition by
372 GAL4: structure of a protein-DNA complex. *Nature* 356:408-414.

- 373 18. Giniger E, Varnum SM, Ptashne M. 1985. Specific DNA binding of GAL4, a
374 positive regulatory protein of yeast. *Cell* 40:767-774.
- 375 19. Todd RB, Andranopoulos A. 1997. Evolution of a fungal regulatory gene family:
376 the Zn(II)₂Cys₆ binuclear cluster DNA binding motif. *Fungal Genet* 21:388-450.
- 377 20. Chang, PK. 2003. The *Aspergillus parasiticus* protein AFLJ interacts with the
378 aflatoxin pathway-specific regulator AFLR. *Molecul Genet Genomics*
379 268:711-719.
- 380 21. Vigneshwaran N, Ashtaputre NM, Varadarajan PV, Nachane RP, Paralikar KM,
381 Balasubramanya RH. 2007. Biological synthesis of silver nanoparticles using the
382 fungus *Aspergillus flavus*. *Mater Lett* 61:1413-1418.
- 383 22. Theis T, Marx F, Salvenmoser W, Stahl V, Meyer V. 2005. New insights into the
384 target site and mode of action of the antifungal protein of *Aspergillus giganteus*.
385 *Res Microbiol* 156:47-56.
- 386 23. Sambrook J, Russell DW. 2001. *Molecular Cloning: A Laboratory Manual*. third
387 ed. Vols. 1, 2 and 3. Cold Spring Harbor Laboratory Press, New York (2100 p.,
388 soft cover. SDS. ISBN-10 Cold Spring Harbor).
- 389 24. Wiegand I, Hilpert K, Hancock RE. 2008. Agar and broth dilution methods to
390 determine the minimal inhibitory concentration (MIC) of antimicrobial
391 substances. *Nat Protoc* 3:163–175.
- 392 25. Zhou GH, Chen YJ, Kong Q, Ma YX, Liu Y. 2017. Detoxification of Aflatoxin
393 B1 by *Zygosaccharomyces rouxii* with Solid State Fermentation in Peanut Meal.
394 *Toxins* 9:42-51.

- 395 26. Kong Q, Chi C, Yu JJ, Shan SH, Li QY, Li QT, Guan B, Nierman WC, Bennett
396 JW. 2014. The inhibitory effect of *Bacillus megaterium* on aflatoxin and
397 cyclopiazonic acid biosynthetic pathway gene expression in *Aspergillus flavus*.
398 *Appl Microbiol Biot* 98:5161-5172.
- 399 27. Alberts JF, Gelderblom WCA, Botha A, Vanzyl WH. 2009. Degradation of
400 aflatoxin B₁ by fungal laccase enzymes. *Int J Food Microbiol* 135:47-52.
- 401 28. Costa SJ, Almeida A, Castro A, Domingues L, Besir H. 2013. The novel Fh8 and
402 H fusion partners for soluble protein expression in *Escherichia coli*: a comparison
403 with the traditional gene fusion technology. *Appl Microbiol Biot* 97:6779-6791.
- 404 29. Douillard FP, O'Connell-Motherway M, Cambillau C, van Sinderen D. 2011.
405 Expanding the molecular toolbox for *Lactococcus lactis*: construction of an
406 inducible thioredoxin gene fusion expression system. *Microb Cell Fact* 10:66.
- 407 30. Schückerl J, Rylott EL, Grogan G, Bruce NC. 2012. A gene-fusion approach to
408 enabling plant cytochromes p450 for biocatalysis. *Chembiochem* 13:2758-2763.
- 409 31. Terpe K. 2003. Overview of tag protein fusions: from molecular and biochemical
410 fundamentals to commercial systems. *Appl Microbiol Biot* 60:523–533.
- 411 32. Lilie H, Schwarz E, Rudolph R. 1998. Advances in refolding of proteins
412 produced in *E. coli*. *Curr Opin Biotech* 9:497-501.
- 413 33. Pal G, Srivastava S. 2014. Cloning and heterologous expression of p1nE, -F, -J
414 and -K genes derived from soil metagenome and purification of active plantaricin
415 peptides. *Appl Microbiol Biot* 98:1441-1447.
- 416 34. Carvalho AO, Gomes VM. 2009. Plant defensins-prospects for the biological

417 functions and biotechnological properties. *Peptides* 30:1007-1020.
418 35. Saberwal G, Nagaraj R. 1994. Cell-lytic and antibacterial peptides that act by
419 perturbing the barrier function of membranes: facets of their conformational
420 features, structure-function correlations and membrane-perturbing abilities.
421 *BBA-Rev Biomembranes* 1197:109-131.

422

423

424

425

426

427

428

429

430

431

432

433

434

435

436

437

438

439

440

441

442 **TABLE 1** The MICs and MBCs of fusion protein DN-AflR and DN

	Concentrations ($\mu\text{g ml}^{-1}$)							MIC	MBC
	30	50	100	150	400	600	900	($\mu\text{g/ml}$)	($\mu\text{g/ml}$)
DN-AflR	+	+	+	-	-	-	-	150	400
DN	+	+	+	+	+	-	-	600	>900
Negative control	+	+	+	+	+	+	+	/	/

443 Negative control: no inhibitory protein.

444 +: observed fungal growth.

445 -: no fungal growth observed.

446 /: no inhibition.

447

448

449

450

451

452

453

454

455

456

457 **TABLE 2** The basic properties prediction of DN-AflR

Number of amino acids	36
Theoretical pI	8.33
Formula	$C_{146}H_{250}N_{50}O_{54}S_6$
Total number of atoms:	506
Aliphatic index	40.83
Total number of negatively charged residues (Asp+Glu)	4
Total number of positively charged residues (Arg+Lys)	6
Grand average of hydropathicity (GRAVY)	-0.581

458 Basic informations were analyzed by ExPASy (<http://web.expasy.org/protparam/>).

459

460

461

462

463

464

465

466

467

468

469 Figure legends:

470 **FIG 1** Molecular modified fragments and characteristics of *E. coli* expression plasmid
471 *dn-aflR-pet32a*. (A) The chemical formula and base sequences of DN. (B) The
472 aflatoxin biosynthetic pathway and clustered genes, AflR binding site (black area) and
473 intergenic region. (C) Construction of expression plasmid. DNA fragment was
474 digested with Hind III and EcoR I, and inserted into downstream of the thioredoxin
475 (Trx) and then ligated with T4 DNA ligase. DN-AflR was expressed as a fusion
476 protein with Trx and 6His. Ar, an ampicillin resistance gene. (D) Base composition of
477 the inserted fusion gene (thick base) containing genes encoding DN (under line) and
478 zinc finger cluster protein (double line). 6His tag, Trx tag and unique restriction sites
479 (over line) were also indicated.

480 **FIG 2** Effects of DN on mycelia morphology of *A. flavus*. (A), (B), (C), (D): TEM;
481 (E), (F), (G), (H): SEM; (A), (B), (E), (F): Control groups; (C), (D), (G), (H): DN
482 treatment groups.

483 **FIG 3** SDS-PAGE analyzed the expression of DN-AflR. (A) M: molecular weight
484 marker (Takara). Lanes 1 and 2: protein bands of *dn-aflR-pET32a* expression. Lane 3:
485 protein band of empty pET32a expression. Lanes 4, 5 and 6: negative control (before
486 inducted). The position of the fusion protein was indicated with an arrowhead. (B)
487 Analysis of purified fusion protein DN-AflR. M: marker. Lane 1: expressed
488 supernatant after ultrasonic breaking. Lane 2: precipitate after 8mM urea dissolved.

489 Lanes 3, 4 and 5: 50 mM imidazole buffer band, 100 mM imidazole buffer band and
490 300mM imidazole buffer band, respectively. Lanes 6 and 7: 200mM imidazole elution
491 buffer band. The position of the purified protein was indicated with an arrowhead.

492 **FIG 4** Anti- *A. flavus* activity and degradation of AFB₁. (A) Plate a: treated with DN.
493 Plate b: treated with 200 mM imidazole. Plate c: control group with no treatment.
494 Plates d, e and f: treated with DN-AflR, the circle diameters of them were around 24,
495 19 and 21mm, respectively. (B) The abscissa represented the final concentration of
496 DN (solid line) and DN-AflR (dotted line), the ordinate (content of AFB₁ without any
497 treatment as 100%. The residual rates of the final concentrations of inhibitory proteins
498 in the three experimental groups, they were 30, 60 and 90 ug mL⁻¹, respectively.

499 **FIG 5** Predicted structure of DN-AflR. (A) Secondary structure. Line 1:
500 Transmembrane helix preference (THM index). Line 2: Beta preference (BET index).
501 Line 3: Modified hydrophobic moment index (INDA index). (B) Spatial structure of
502 DN-AflR. Marked position in circle: zinc finger structure. (C) Structure of GAL4.
503 Marked position in circle: zinc finger structure. (D) Zinc finger structure.

504

505

506

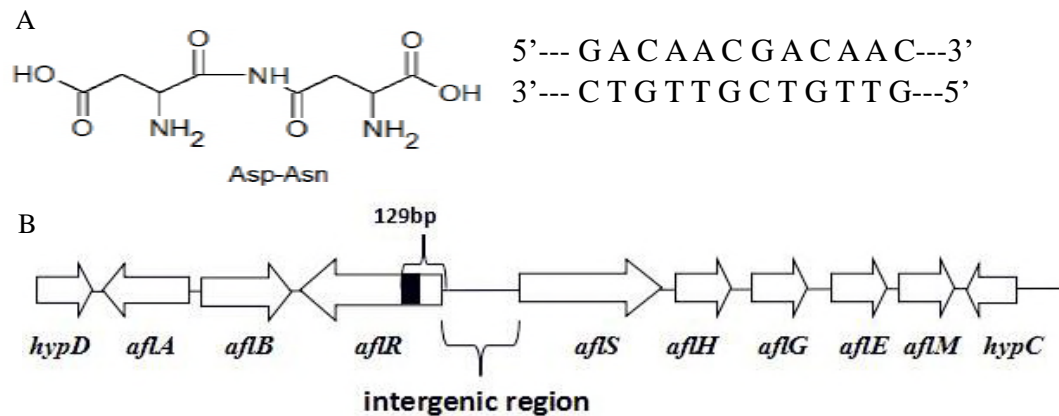
507

508

509

510

511



512

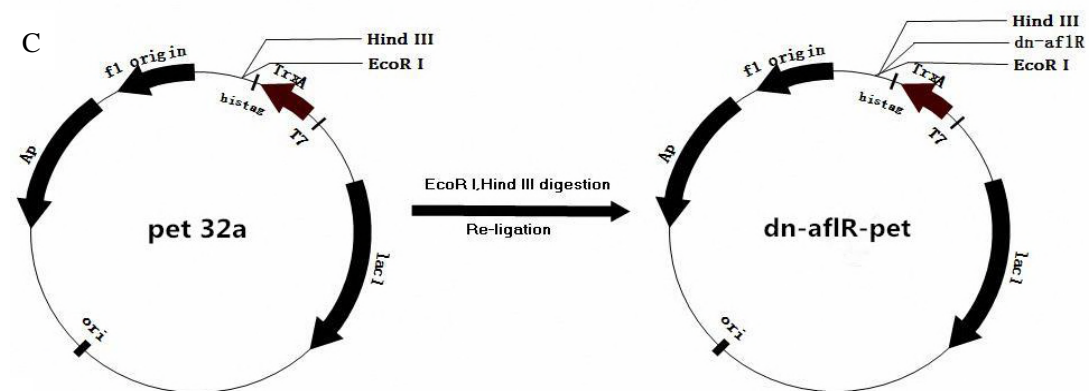
513

514

515

516

517



D

T7 promoter → Lac operator Xba I

TAATACGACTCACTAGGGGAATTGTGAGCGGATAACAATTCCCCTCTAGAAATAATTTTGT

rbs Trx.Tag Msc I

TAACTTTAAGAAGGAGATATACATATGAGC.....315bp....CTGGCCGGTCTGGTTCTGGCCAT

His.Tag thrombin

ATGCACCATCATCATCATTCTTCTGGTCTGGTGCCACGCGGTTCTGGTAT

S.Tag Nsp V Bgl II Kpn I

GAAAGAAACCCTGCTAAATTCGAACGCCAGCACATGGACAGCCCAGATCTGGGTACC

Nco I EcoR V BamHI EcoR I

GACGACGACGACAAGGCCATGGCTGATATCGGATCCGAATTCGACAACGACAAC
Asp Asn Asp Asn

linker

TCTCCAGGTTCC TGTACGAGTTGTGCCAGCTCAAAAGTGCATGCACCAAGGAGAAA
Cys Cys Cys

Hind III

CCGGCCTGTGCTCGGTGTATCGAACGTGGTCTTGCCTGTAAGCTTGAGCTCCGTCGACA
Cys Cys Cys

His.Tag

AGCTTGCGGCCGCACTCGAGCACCACCACCACCAC

518 FIG 1 Molecular modified fragments and characteristics of *E. coli* expression plasmid

519 dn-aflR-pet32a. (A) The chemical formula and base sequences of DN. (B) The
520 aflatoxin biosynthetic pathway and clustered genes, AflR binding site (black area) and
521 intergenic region. (C) Construction of expression plasmid. DNA fragment was
522 digested with Hind III and EcoR I, and inserted into downstream of the thioredoxin
523 (Trx) and then ligated with T4 DNA ligase. DN-AflR was expressed as a fusion
524 protein with Trx and 6His. Ar, an ampicillin resistance gene. (D) Base composition of
525 inserted fusion gene (thick base) containing genes encoding DN (under line) and zinc
526 finger cluster protein (double line). 6His tag, Trx tag and unique restriction sites (over
527 line) were also indicated.

528

529

530

531

532

533

534

535

536

537

538

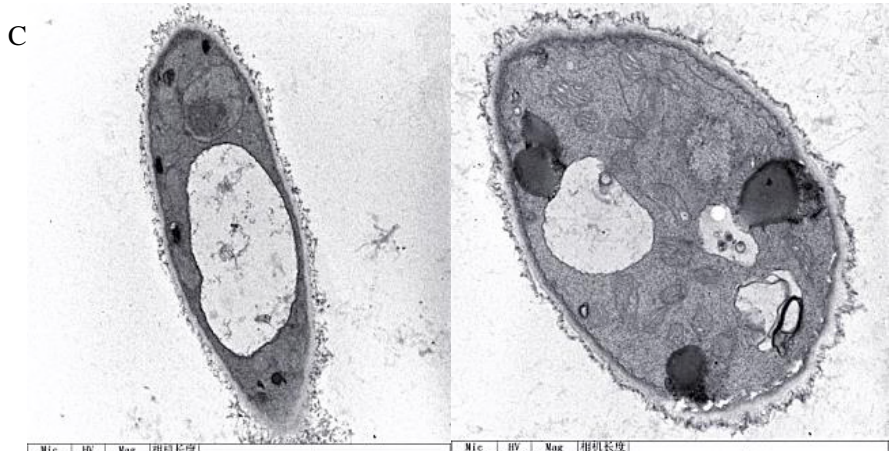
539

540



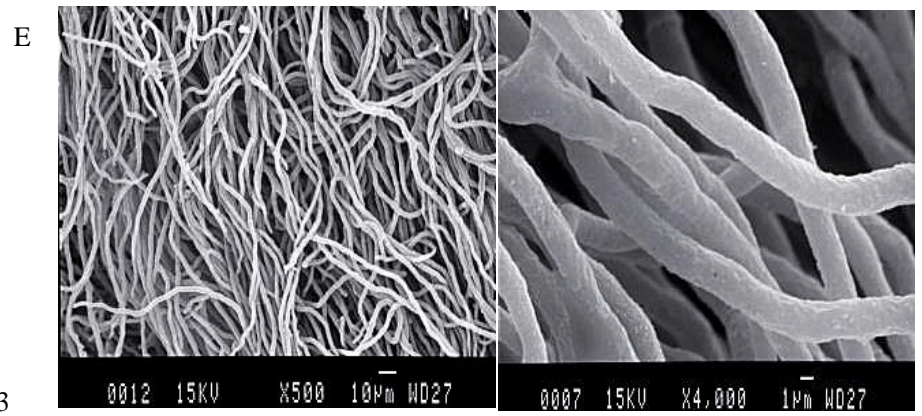
541

Mic	HV	Mag	相机长度
EM-1200	80 kV	30000 x	—1 μm—
EM-1200	80 kV	60000 x	—500 nm—



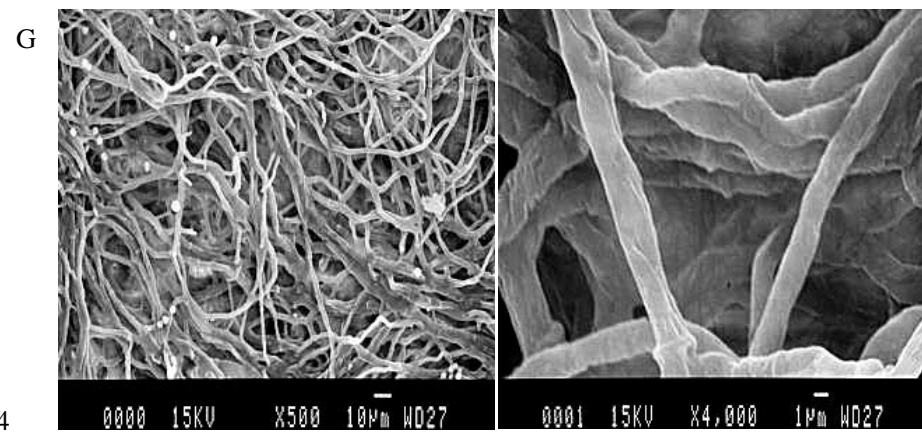
542

Mic	HV	Mag	相机长度
EM-1200	80 kV	30000 x	—1 μm—
EM-1200	80 kV	30000 x	—1 μm—



543

0012	15KV	X500	10μm	WD27
0007	15KV	X4,000	1μm	WD27



544

0000	15KV	X500	10μm	WD27
0001	15KV	X4,000	1μm	WD27

545 **FIG 2** Effects of DN on mycelia morphology of *A. flavus*. (A), (B), (C), (D): TEM;
546 (E), (F), (G), (H): SEM; (A), (B), (E), (F): Control groups; (C), (D), (G), (H): DN
547 treatment.

548

549

550

551

552

553

554

555

556

557

558

559

560

561

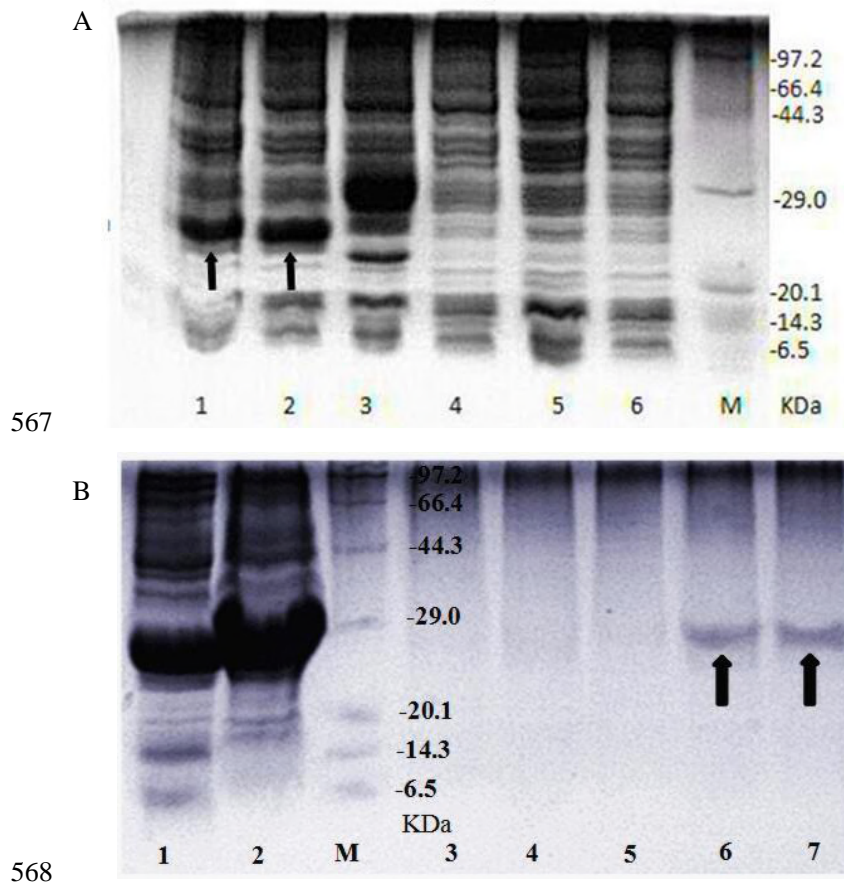
562

563

564

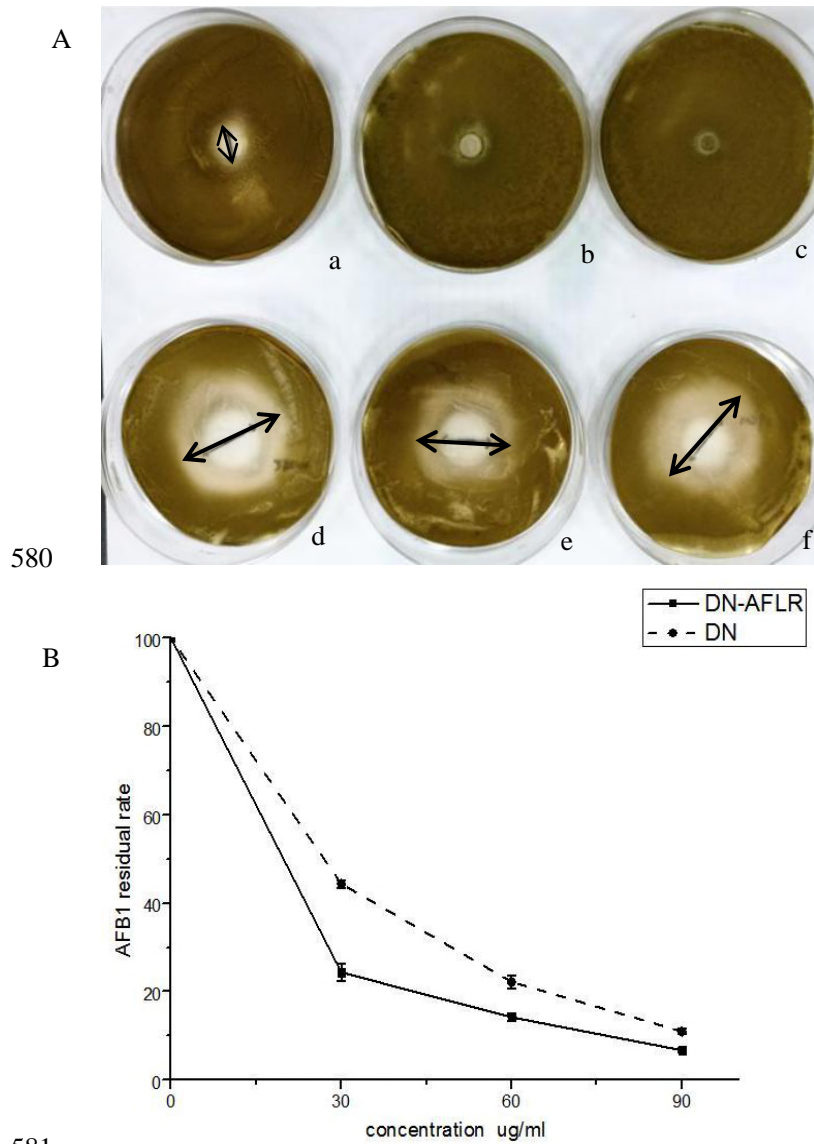
565

566



569 **FIG 3** SDS-PAGE analyzed the expression of DN-AflR. (A) M: molecular weight
570 marker (Takara). Lanes 1 and 2: protein bands of dn-aflR-pET32a expression. Lane 3:
571 protein band of empty pET32a expression. Lanes 4, 5 and 6: negative control (before
572 induced). The position of the fusion protein was indicated with an arrowhead. (B)
573 Analysis of purified fusion protein DN-AflR. M: marker. Lane 1: expressed
574 supernatant after ultrasonic breaking. Lane 2: precipitate after 8 mM urea dissolved.
575 Lanes 3, 4 and 5: 50 mM imidazole buffer band, 100 mM imidazole buffer band and
576 300mM imidazole buffer band, respectively. Lanes 6 and 7: 200 mM imidazole
577 elution buffer band. The position of the purified protein was indicated with an
578 arrowhead.

579



581

582 **FIG 4** Anti- *A. flavus* activity and degradation of AFB₁. (A) Plate a: treated with DN.

583 Plate b: treated with 200 mM imidazole. Plate c: control group with no treatment.

584 Plates d, e and f: treated with purified fusion protein DN-AfIR, the circle diameter of

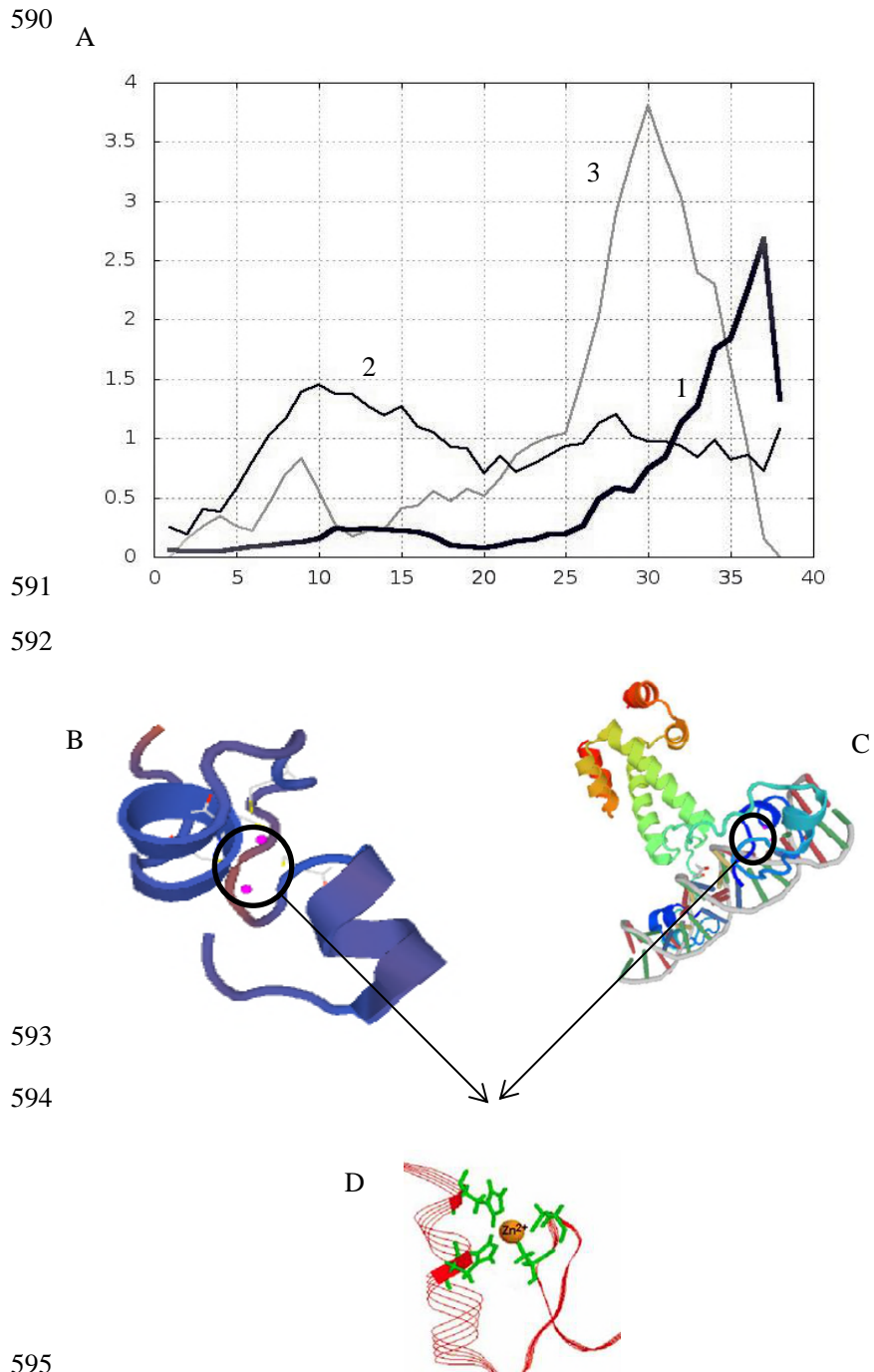
585 them was around 24, 19 and 21mm, respectively. (B) The abscissa represented the

586 final concentration of DN (solid line) and DN-AfIR (dotted line), the ordinate (content

587 of AFB₁ without any treatment as 100%. The residual rates of the final concentrations

588 of inhibitory proteins in the three experimental groups, they were 30, 60 and 90 ug

589 mL⁻¹, respectively.



596 **FIG 5** Predicted structure of DN-AfIR. (A) Secondary structure. Line 1:
597 Transmembrane helix preference (THM index). Line 2: Beta preference (BET index).
598 Line 3: Modified hydrophobic moment index (INDA index). (B) Spatial structure of
599 DN-AfIR. Marked position in circle: zinc finger structure. (C) Structure of GAL4.
600 Marked position in circle: zinc finger structure. (D) Zinc finger structure.